Journal of Power Sources 196 (2011) 6232–6237

Contents lists available at ScienceDirect

Journal of Power Sources

journal homepage: www.elsevier.com/locate/jpowsour

Short communication

Highly dispersed Pd nanoparticles supported on 1,10-phenanthroline-functionalized multi-walled carbon nanotubes for electrooxidation of formic acid

Zhengyu Bai[a], Yuming Guo[a], Lin Yang[a,*], Lei Li[b], Wujv Li[c], Pengle Xu[a], Chuangang Hu[a], Kui Wang[a]

[a] College of Chemistry and Environmental Science, Henan Normal University, Key Laboratory of Green Chemical Media and Reactions, Ministry of Education, Xinxiang 453007, PR China
[b] School of Chemistry and Chemical Technology, Shanghai Jiao Tong University, Shanghai 200240, PR China
[c] Luohe Vocational Technology College, Luohe 462002, PR China

ARTICLE INFO

Article history:
Received 5 March 2011
Accepted 9 March 2011
Available online 25 March 2011

Keywords:
Functionalization
Supramolecular π–π stacking
Palladium
Formic acid oxidation
Active sites

ABSTRACT

Functionalization step is generally prerequisite to immobilize metal nanoparticles on multi-walled carbon nanotubes (MWCNTs) for production of a high efficient electrocatalyst. We herein report a novel method to functionalize MWCNTs with 1,10-phenanthroline (phen-MWCNTs) as a catalyst support for Pd nanoparticles. Raman spectroscopic analysis results reveal that this phen functionalization method can preserve the integrity and electronic structure of MWCNTs and provide the highly effective functional groups on the surface for Pd nanoparticles. According to the transmission electron microscopy (TEM) measurements, the as-prepared Pd nanop articles are evenly deposited on the surface of the phen-MWCNTs without obvious agglomeration, and the average particle size of the Pd nanoparticles is 2.3 nm. Electrochemical measurements demonstrate that the as-prepared Pd/phen-MWCNTs catalyst has a better electrocatalytic activity and stability for the oxidation of formic acid than Pd catalyst on acid-treated MWCNTs. It is concluded that the as-prepared Pd/phen-MWCNTs would be a potential candidate as an anode electrocatalyst in direct formic acid fuel cell (DFAFC).

1. Introduction

Direct formic acid fuel cell (DFAFC) is considered to be a promising system for automotive and portable electronic applications owing to its high energy density and low operating temperature [1–3]. DFAFC has advantages over the direct methanol fuel cell because it can achieve a higher power density and formic acid is nontoxic, although the energy density of methanol is higher than that of formic acid [4,5]. However, the commercial application of the DFAFC is still hindered by several issues including its insufficient activity and high cost of anode catalysts [6,7]. To solve these problems, tremendous efforts have been made to find catalysts with high activity, stability, and low cost. Recently, Pd and Pd derivatized-catalysts have been shown to perform better in formic acid oxidation than Pt derivatized-catalysts [8,9]. Meanwhile, the ideal support with large surface area, good conductivity and strong adsorption of metals shows the ability to improve the dispersion of metal nanoparticles, and thereby can enhance the utilization and efficiency of the noble metal electrocatalysts [10,11].

Because of the significant influence of the support on the dispersion and size of catalyst nanoparticles and thereby the catalytic activity and stability of the catalysts, the choice of a suitable support is one of the key factors affecting the performance of the catalysts [12,13]. In this regard, multi-walled carbon nanotubes (MWCNTs) are considered to be the ideal electrocatalyst support because they possess a large surface area, good thermal and chemical stability as well as great electrical conductivity [14]. However, the anchored metal nanoparticles tend to aggregate together, and lead to reduction in electrochemically active surface areas (EAS) due to the inefficient binding sites on the pristine MWCNTs surface for anchoring precursor metal ions or metal nanoparticles. Therefore, functionalization of MWCNTs is generally prerequisite for further applications [15]. Although the acid-oxidized (AO) process is frequently used, it is too complex and may even impair the mechanical properties of MWCNTs [16]. Recently, some alternative effective methods have been developed to functionalize MWCNTs [17]. For example, 1-aminopyrene and ionic-liquid polymer has been used to functionalize the MWCNTs by introducing the functional groups onto the surface of MWCNTs [18,19]. However, it is still a great challenge to control the deposition, distribution, and size of metal nanoparticles supported on MWCNTs.

* Corresponding author. Tel.: +86 373 3326058; fax: +86 373 3328507.
E-mail address: yanglin1819@163.com (L. Yang).

0378-7753/$ – see front matter.
doi:10.1016/j.jpowsour.2011.03.020

Nitrogen doping onto the support can effectively increase the active sites of the electrocatalysts. With the introduction of the nitrogen, Pd nanoparticles can be homogeneously anchored onto the support, leading to the generation of MeN*x* (Me Co, Fe) active sites and thereby enhancing the electrocatalytic activity and utilization efficiency of the catalyst. We have previously prepared a Pd/PPy-XC-72 catalyst with hollow nanospheric Pd being entrapped into the structure of PPy via a very simple chemical reduction method [20].

In the present study, 1,10-phenanthroline (phen) with N atom is used as a functionalization reagent for MWCNTs to prepare a Pd electrocatalyst through a facile process at room temperature. The results show that the phen-MWCNTs demonstrate to be a good support for the electrocatalyst with smaller particle size and better dispersion. Compared with the AO-MWCNTs, the phen-MWCNTs possess a structure of supramolecular π–π stacking, which is able to preserve the integrity and the electronic structure of the MWCNTs. Most important is that the presence of N atoms in phen makes the Pd nanoparticles homogeneously anchored onto the phen-MWCNTs, produce some active Me–N sites, and generate a good electrocatalytic activity and stability for the formic acid oxidation.

2. Experimental

2.1. Phen-functionalization and acid-treatment of MWCNTs

MWCNTs was noncovalently functionalized with phen. In brief, 200 mg pristine MWCNTs were sonicated in 100 mL ethanol containing 50 mg phen for 1 h and stored at room temperature overnight. Subsequently, the as-functionalized MWCNTs were collected by filtration and washed several times, then dried at 40 °C under vacuum for 12 h. The as-functionalized MWCNTs with phen were denoted as phen-MWCNTs. As a comparison, MWCNTs were also functionalized by a conventional acid treatment. Briefly, MWCNTs were pretreated in boiled mixed acid solution (H_2SO_4:HNO_3 in 1:1, v/v ratio) for 8 h, then washed with double distilled water (DD water) and dried at 40 °C under vacuum for 12 h. The resultant acid-treated MWCNTs were denoted as AO-MWCNTs.

2.2. Synthesis of Pd/MWCNTs electrocatalyst

To deposit the Pd nanoparticles on phen-MWCNTs, 40 mg pretreated MWCNTs were added into 100 mL ethanol–water (1:1, v/v) solution, and ultrasonically treated for 30 min. Subsequently, $PdCl_2$ (10 mg Pd in 5 mL DD H_2O) aqueous solution was added into the system and the pH was adjusted to 10 using 0.5 M NaOH solution under moderate stirring for 2 h, then stored at room temperature overnight. A freshly prepared KBH_4 solution (100 mg in 100 mL DD water) was added dropwise into the above solution under moderate stirring for 2 h, and then the stirring was continued for another 10 h to make sure the completely reduction of Pd^{2+}. The whole process was operated at room temperature. Finally, the product was collected by filtration and washed several times, then dried at 40 °C under vacuum for 12 h, and Pd/phen-MWCNTs electrocatalyst was obtained.

For a comparison, Pd electrocatalysts on acid-treated MWCNTs (Pd/AO-MWCNTs) were also prepared using similar procedures as described above.

2.3. Characterization of Pd/MWCNTs electrocatalyst

The morphology of the catalysts was determined by JEOL-100CX high resolution transmission electron microscopy (HR-TEM) operated at 200 kV. Samples were ultrasonicated and dispersed in ethanol. A drop of the suspension was then deposited on a lacey carbon grid and dried in air. Thermogravimetric analysis (TGA) was performed on a NETZSCH STA 449C. Powder X-ray diffraction (XRD) pattern was recorded on D/max-2200/PC X-ray diffractometer with Cu Kα radiation source. The surface structure of the MWCNTs was examined by Raman spectroscopy (Renishaw Rm-1000), using He/Ne laser with a wavelength of 457.5 nm.

2.4. Electrochemical behavior of Pd/MWCNTs electrocatalyst

Cyclic voltammetry measurements were carried out in a three-electrode cell by using Solartron 1287 electrochemical test system (Solartron Analytical, England). A glassy carbon disk (3 mm o.d.) coated with catalyst was used as the working electrode, a platinum foil (1 cm^{-2}) as the counter-electrode, and an Ag/AgCl electrode as the reference. The metal loading of the as-prepared catalysts on glassy carbon electrode is 386 μg cm^{-2}. 0.5 M H_2SO_4 aqueous solution was used as electrolyte for hydrogen oxidation measurements, and 0.5 M HCOOH containing 0.5 M H_2SO_4 for formic acid oxidation measurements, respectively. High-purity N_2 was bubbled into the electrolyte during the experiments. All electrochemical measurements were performed at 25 ± 1 °C.

Electrochemical CO stripping voltammograms were obtained by oxidizing preadsorbed CO (COad) in 0.5 M H_2SO_4 at a scan rate of 20 mV s^{-1}. CO was purged through 0.5 M H_2SO_4 for 30 min to allow complete adsorption of CO onto the catalyst. The working electrode was stayed at 0.1 V (*vs.* Ag/AgCl), and excess CO in the electrolyte was removed by purging with high-purity N_2 for 30 min. The amount of COad was evaluated by integrating the COad stripping peak and correcting for the capacitance of the electric double-layer. The activity of the catalysts in the oxidation of formic acid was evaluated in a solution containing 0.5 M H_2SO_4 and 0.5 M HCOOH, and cyclic voltammetry measurement was performed by applying a linear potential scan at a sweep rate of 50 mV s^{-1}.

3. Results and discussion

In this work, Pd nanoparticles supported on phen-MWCNTs were prepared through a facile process at room temperature. The formation mechanism of Pd/phen-MWCNTs electrocatalyst may be as follows (Scheme 1). Firstly, 1,10-phenanthroline could form an adsorption layer on the surface of the MWCNTs by supramolecular π–π stacking. Secondly, Pd^{2+} was added into the system to coordinate with phen. Thirdly, the Pd^{2+} was *in situ* reduced to Pd nanoparticles, at the same time, the active Pd–N sites could be formed. Herein, the stabilizing effect of the phen may be attributed to its bifunctional features, which can act as an interlinker between the surface of the MWCNTs and the nanoparticles. On the one hand, the aryl on the one terminal maybe noncovalently interact with the six-membered carbon rings of the MWCNTs by π–π stacking. On the other hand, the C–N groups on the other terminal maybe adsorb Pd^{2+} via electrostatic interactions, followed by the *in situ* formation of the corresponding nanoparticles on the MWCNTs [17].

Fig. 1 shows the transmission electron microscopy (TEM) images and the size frequency curve of the resulting sample from the typi-

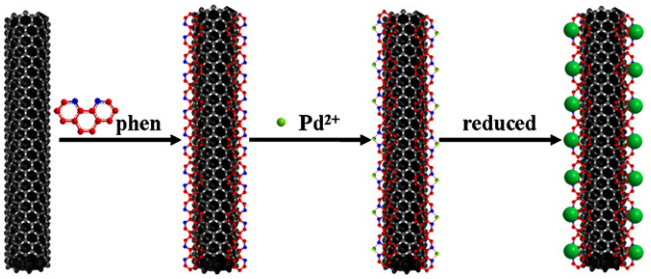

Scheme 1. The formation mechanism of the Pd/phen-MWCNTs catalyst.

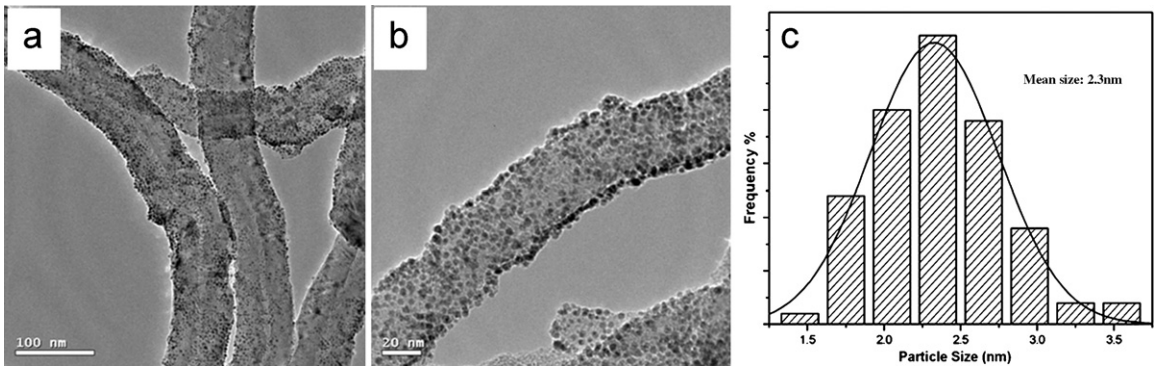

Fig. 1. TEM images and corresponding size distribution of the synthesized Pd/phen-MWCNTs catalysts.

cal experiment. From Fig. 1a, Pd nanoparticles with a small particle size are evenly deposited on the surface of the phen-MWCNTs. The nanoparticles diameters from the amplificatory TEM image (Fig. 1b) range from 1.4 to 3.6 nm and the mean size calculated by the log-normal distribution is 2.3 nm (Fig. 1c). To investigate the influence of the functionalization methods of the MWCNTs on the formation of Pd nanoparticles, a control experiment was carried out under the same conditions described as the typical experiment, apart from the AO-MWCNTs as the support. Fig. 2 shows the TEM image and the size frequency curve of the Pd nanoparticles supported on the AO-MWCNTs. From Fig. 2a, Pd nanoparticles poorly distribute and larger than those on the phen-MWCNTs. It is likely due to the ununiform defects generated on the surface of the MWCNTs by the AO treatment. When Pd nanoparticles are deposited on the AO-MWCNTs, the particles tend to deposit on these localized defect sites, leading to the poor dispersion and extensive aggregation. In contrast, immobilization of phen on the surface of the MWCNTs produce the uniform distribution of the C–N sites, which can serve as the functional groups for the self-assembly of Pd precursors on the surface of the MWCNTs. Therefore, Pd nanoparticles with a much more uniform size and distribution could be formed, and might contribute to the good electrocatalytic activity and stability for the formic acid oxidation.

In order to confirm the existence of 1,10-phenanthroline, the as-prepared Pd/phen-MWCNTs and pure 1,10-phenanthroline monohydrate were analyzed by TGA under the protection of N_2 at a heating rate of $10^{\circ}\,min^{-1}$ from 30 to 700 °C. The obtained TGA curves are shown in Fig. 3. The TGA curve of the pure 1,10-phenanthroline monohydrate shows a two-step weight loss (Fig. 3a). The first step (100–110 °C) is attributed to the loss of the crystal water. The second step, which starts at 250 °C and ends at 340 °C, corresponds to the degradation of 1,10-phenanthroline. It is evident that 1,10-phenanthroline can be decomposed completely. From Fig. 3b, the TGA curve of the Pd/phen-MWCNTs catalyst shows the same process of weight loss compared to pure 1,10-phenanthroline monohydrate. Overall, the results indicate that the phen-MWCNTs are successfully prepared and the content of phen is about 8%.

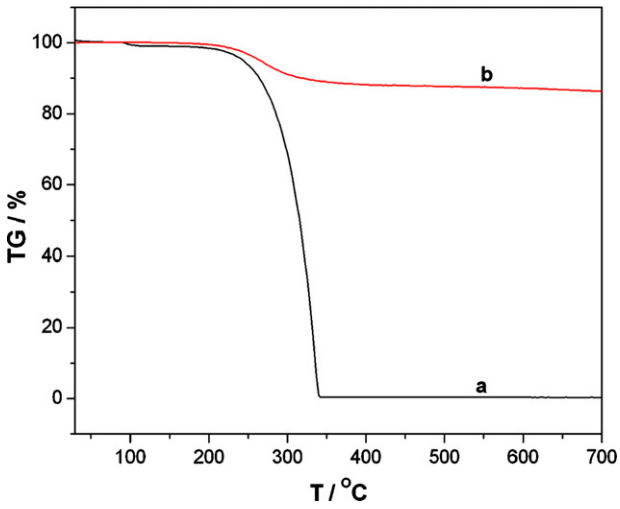

Fig. 3. TGA curves of pure 1,10-phenanthroline monohydrate (a) and as-prepared Pd/phen-MWCNTs (b) under the protection of N_2.

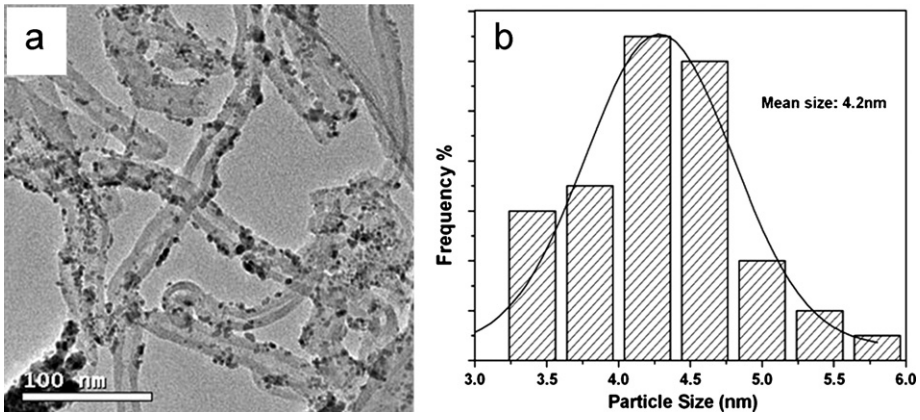

Fig. 2. TEM images and corresponding size distribution of the Pd/AO-MWCNTs catalysts.

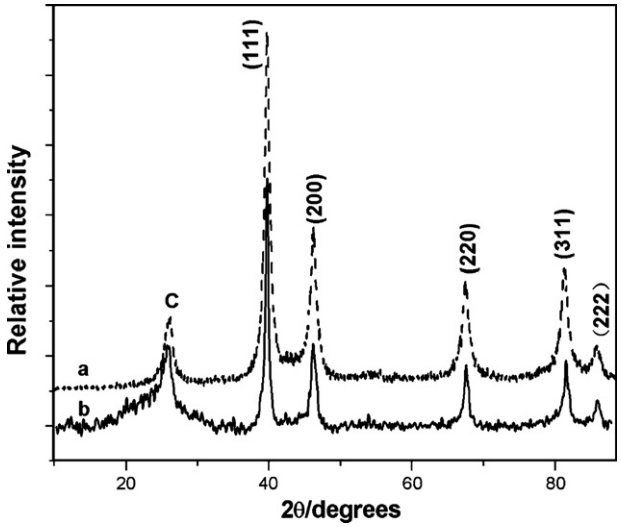

Fig. 4. XRD patterns of the as-prepared Pd/phen-MWCNTs (a) and Pd/AO-MWCNTs (b).

Fig. 4 shows the XRD patterns of the as-prepared Pd/phen-MWCNTs and Pd/AO-MWCNTs, respectively. Five peaks at 39.8°, 46.3°, 67.6°, 81.9° and 86.1° are characteristics of face-centered-cubic (fcc) crystalline Pd, which are corresponding to the facets (1 1 1), (2 0 0), (2 2 0), (3 1 1) and (2 2 2), respectively, except for the characteristic peak of the MWCNTs support around 25°. Obviously, different functionalization methods of the MWCNTs support have no significant influence on the crystalline form of Pd nanoparticles. In addition, the full width at half maximum (FWHM) of the diffraction peaks of the Pd/phen-MWCNTs is wider than that of the Pd/AO-MWCNTs, indicating the smaller particle size of the Pd nanoparticles supported on the phen-MWCNTs. This is in agreement with the results of the HR-TEM and size distribution analysis.

The Raman spectroscopy was used to study the surface structure of the MWCNTs. Fig. 5. displays the Raman spectra of AO-MWCNTs, pristine MWCNTs, and phen-MWCNTs, respectively. The peak at a.c. 1360 cm^{-1} is assigned to the A_{1g} breathing mode of the disordered graphite structure (D band), while the high-frequency peak at a.c. 1590 cm^{-1} is assigned to the E_{2g} stretching mode of the graphite (G band). The G band reflects the structure of the sp^2 hybridized carbon atom. Thus the extent of the modification or defects in MWCNTs could be evaluated by the intensity ratio of the D- and G-bands. The I_D/I_G ratio is 0.98, 0.72, and 0.59 for AO-MWCNTs, pristine MWCNTs, and phen-MWCNTs, respectively. A clear trend can be observed that the AO-MWCNTs have the largest I_D/I_G ratio. The I_D/I_G ratio of the phen-MWCNTs is similar to that of the pristine MWCNTs, indicating that the immobilization of phen on the sidewalls of MWCNTs has no detrimental effect on the surface structure of CNTs. In contrast, the I_D/I_G ratio of AO-MWCNTs is much higher than of the pristine MWCNTs, indicating that the harsh acid treatment produces carboxylic acid sites on the surface, causing severe structural damage of MWCNTs. In comparison, the phen functionalization method preserves the integrity and electronic structure of the MWCNTs and provides highly effective functional groups on the surface of MWCNTs, which contribute to the subsequent deposition of Pd nanoparticles with a much more uniform size and distribution.

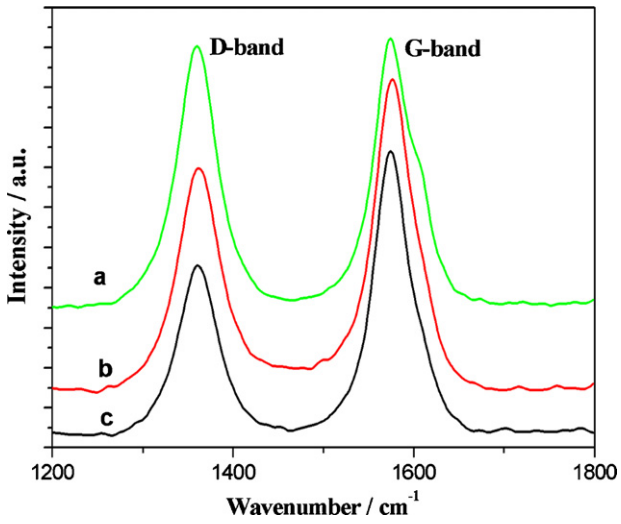

Fig. 5. Raman spectra of (a) AO-MWCNTs, (b) pristine MWCNTs and (c) phen-MWCNTs.

The electrochemical behavior of different catalysts were recorded by cyclic voltammetry (CV) measurement, which was performed in 0.5 M H_2SO_4 electrolyte at a scan rate of 20 mV s^{-1}. Fig. 6 shows the cyclic voltammograms obtained with CO adsorbed onto the catalysts (solid curves) and without CO adsorbed (dashed curves), of the as-prepared Pd/phen-MWCNTs and Pd/AO-MWCNTs, respectively. Obviously, the hydrogen adsorption peak of the Pd/phen-MWCNTs is larger than that of the Pd/AO-MWCNTs,

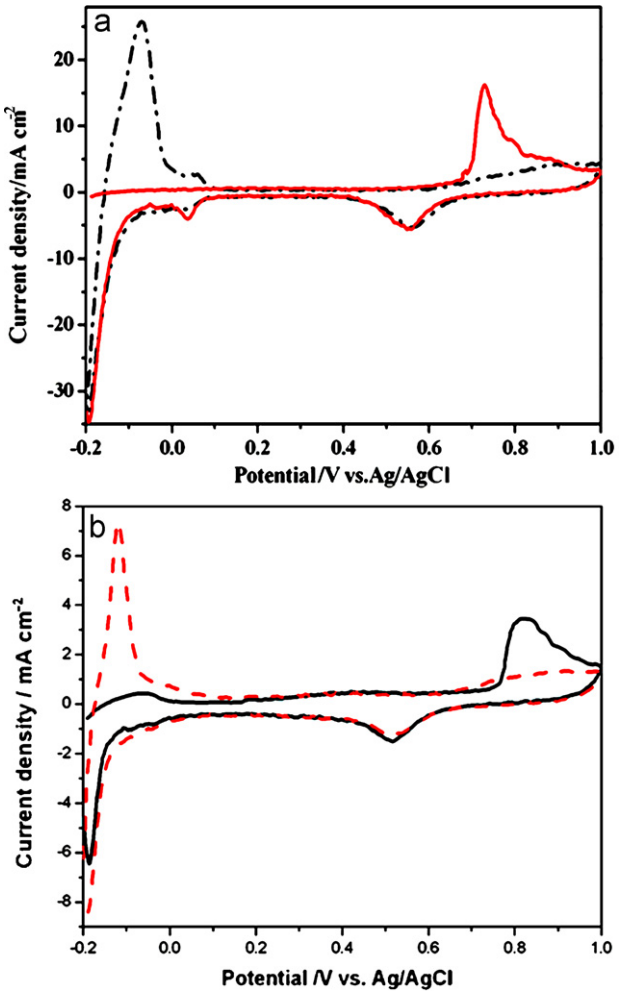

Fig. 6. Cyclic voltammograms for the oxidation of preadsorbed CO of the as-prepared catalysts from (a) Pd/phen-MWCNTs and (b) Pd/AO-MWCNTs on glassy carbon electrode in 0.5 M H_2SO_4 aqueous solution with a scan rate of 20 mV s^{-1} at 25 °C. Dashed curves were CVs for these electrodes without COad.

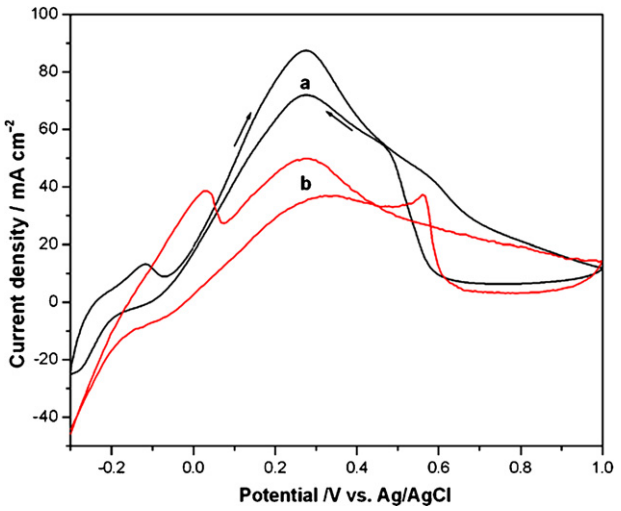

Fig. 7. Cyclic voltammograms of (a) Pd/phen-MWCNTs and (b) Pd/AO-MWCNTs on glassy carbon electrode in 0.5 M H_2SO_4 + 1 M HCOOH aqueous solution with a scan rate of 50 mV s^{-1} at 25 °C.

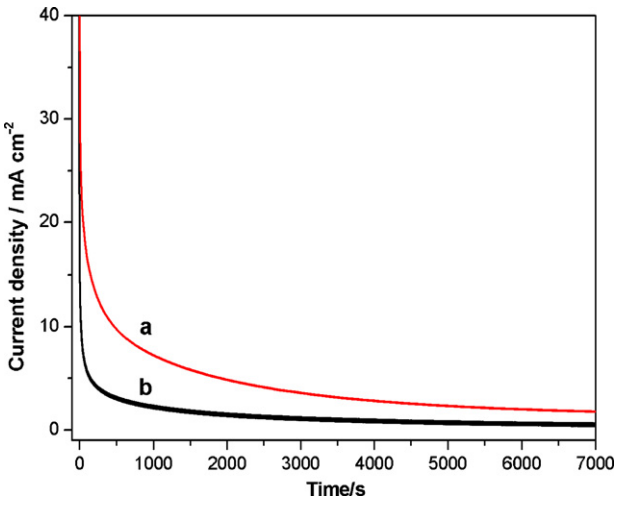

Fig. 8. Chronoamperometric curves of (a) Pd/phen-MWCNTs and (b) Pd/AO-MWCNTs on glassy carbon electrode in 0.5 M H_2SO_4 + 1 M HCOOH aqueous solution at a potential of 0.1 V.

indicating that the Pd/phen-MWCNTs has a higher electrocatalytic activity. The corresponding EAS of the catalyst was obtained from Eq. (1) [21,22]:

$$\mathrm{EAS} = \frac{Q}{G \times 420} \quad (1)$$

where Q is the charge of CO desorption–electrooxidation in microcoulomb (μC), G represents the total amount of Pd (μg) on the electrode, and 420 is the charge required to oxidize a monolayer of CO on the catalyst in μC cm^{-2}. The EAS value of the Pd/phen-MWCNTs catalyst (37.6 m^2 g^{-1}) is much larger than that of the Pd/AO-MWCNTs catalyst (15.7 m^2 g^{-1}), leading to the higher electrocatalytic activity. The larger EAS of the Pd/phen-MWCNTs catalyst might be attributed to the smaller size and better dispersion of the Pd nanoparticles.

The electrocatalytic activities for the formic acid oxidation of the as-prepared electrocatalysts were analyzed by CV measurement in 0.5 M H_2SO_4 + 1 M HCOOH aqueous solution. The CV curves of the Pd/phen-MWCNTs and Pd/AO-MWCNTs catalyst electrodes are displayed in Fig. 7. Two main peaks for the formic acid oxidation in both positive and negative direction are observed at the both electrodes. Clearly, the maximum peak current density of the Pd/phen-MWCNTs catalyst is much higher than that of the Pd/AO-MWCNTs catalyst, demonstrating further the higher catalytic activity of the Pd/phen-MWCNTs catalyst than that of the Pd/AO-MWCNTs catalyst for the formic acid oxidation. Furthermore, comparing with the previous data, the electrocatalytic activity and utilization efficiency of the Pd/phen-MWCNTs catalyst has increased significantly [8,9,23].

In order to compare the electrochemical stability of the as-prepared catalysts for formic acid oxidation, chronoamperometry tests were carried out in 0.5 M H_2SO_4 + 1 M HCOOH aqueous solution at 0.1 V for 7000 s (shown in Fig. 8). Evidently, the Pd/phen-MWCNTs catalyst shows much higher anodic currents and much slower degradation in currents, demonstrating better activity and stability than that of the Pd/AO-MWCNTs catalyst under the same conditions.

4. Conclusions

In conclusion, the Pd/phen-MWCNTs catalyst for the oxidation of formic acid has been prepared through a facile chemical reduction method at room temperature. Herein, phen makes a strong impact on the electrocatalytic activity of the catalyst through the functionalization of the MWCNTs and the formation of the active Pd–N sites. Therefore, the dispersivity and the ESA of the Pd nanoparticles are obviously enhanced in the presence of phen, resulting in better electrocatalytic activity and utilization efficiency of the catalyst. Thus, the as-prepared Pd/phen-MWCNTs should be a good candidate catalyst for DFAFC.

Acknowledgments

This work was financially supported by the Henan Key Proposed Program for Basic and Frontier Research (Grant no. 092300410121), the National Key Basic Research and Development Program of China (Grant no. 2009CB626610), the Innovation Scientists and Technicians Troop Construction Projects of Henan Province and the Dr start-up fund of Henan Normal University.

References

[1] B. Lim, M.J. Jiang, P.H.C. Camargo, E.C. Cho, J. Tao, X.M. Lu, Y.M. Zhu, Y.N. Xia, Science 324 (2009) 1302–1305.
[2] Y.M. Zhu, S.Y. Ha, R.I. Masel, J. Power Sources 130 (2004) 8–14.
[3] S.J. Kang, J. Lee, J.K. Lee, S.Y. Chung, Y. Tak, J. Phys. Chem. B 110 (2006) 7270–7274.
[4] Y.M. Zhu, Z. Khan, R.I. Masel, J. Power Sources 139 (2005) 15–20.
[5] R.S. Jayashree, J.S. Spendelow, J. Yeom, C. Rastogi, M.A. Shannon, P.J.A. Kenis, Electrochim. Acta 50 (2005) 4674–4682.
[6] J. Zhao, P. Wang, W.X. Chen, R. Liu, X. Li, Q.L. Nie, J. Power Sources 160 (2006) 563–569.
[7] R.F. Wang, H. Li, H.Q. Feng, H. Wang, Z.Q. Lei, J. Power Sources 195 (2010) 1099–1102.
[8] X.M. Wang, Y.Y. Xia, Electrochim. Acta 54 (2009) 7525–7530.
[9] Z.Y. Bai, L. Yang, J.S. Zhang, L. Li, J. Lv, C.G. Hu, J.G. Zhou, Catal. Commun. 11 (2010) 919–922.
[10] Z.L. Liu, L. Hong, M.P. Tham, T.H. Lim, H. Jiang, J. Power Sources 161 (2006) 831–835.
[11] X. Wang, Y.W. Tang, Y. Gao, T.H. Lu, J. Power Sources 175 (2008) 784–788.
[12] M. Uchida, Y. Aoyama, M. Tanabe, N. Yanagihara, N. Eda, A. Ohta, J. Electrochem. Soc. 142 (1995) 2572–2576.
[13] B. Rajesh, V. Karthik, S. Karthikeyan, K.R. Thampi, J.M. Bonard, B. Viswanathan, Fuel 81 (2002) 2177–2190.
[14] P.J. Britto, K.S.V. Santhanam, P.M. Ajayan, Bioelectrochem. Bioenerg. 41 (1996) 121–125.
[15] J.F. Lin, V. Kamavaram, A.M. Kannan, J. Power Sources 195 (2010) 466–470.
[16] Y.L. Hsin, K.C. Hwang, C.T. Yeh, J. Am. Chem. Soc. 129 (2007) 9999–10010.
[17] N. Karousis, N. Tagmatarchis, D. Tasis, Chem. Rev. 110 (2010) 5366–5397.
[18] S.Y. Wang, X. Wang, S.P. Jiang, Langmuir 24 (2008) 10505–10512.
[19] B.H. Wu, D. Hu, Y.J. Kuang, B. Liu, X.H. Zhang, J.H. Chen, Angew. Chem. Int. Ed. 48 (2009) 4751–4754.

[20] Z.Y. Bai, L. Yang, L. Li, J. Lv, K. Wang, J. Zhang, J. Phys. Chem. C 113 (2009) 10568–10573.
[21] Y.C. Zhao, X.L. Yang, J.N. Tian, F.Y. Wang, L. Zhan, J. Power Sources 195 (2010) 4634–4640.
[22] M.J. Weaver, S.C. Chang, L.W.H. Leung, X. Jiang, M. Rubel, M. Szklarczyk, D. Zurawski, A. Wieckowski, J. Electroanal. Chem. 327 (1992) 247–260.
[23] Y. Zhu, Y.Y. Kang, Z.Q. Zou, Q. Zhou, J.W. Zheng, B.J. Xia, H. Yang, Electrochem. Commun. 10 (2008) 802–805.